EasyChair Preprint

№ 15719

Control of a VTOL Aircraft Model with Air-Launched Missile Release Impact and Wind Disturbances

Selim Sivrioğlu and Sinan Basaran

EasyChair preprints are intended for rapid dissemination of research results and are integrated with the rest of EasyChair.

January 15, 2025

Control of a VTOL aircraft model with air-launched missile release impact and wind disturbances

Selim Sivrioglu
Department of Mechanical Engineering
Faculty of Engineering
Piri Reis University
Istanbul, Türkiye
ssivrioglu@pirireis.edu.tr

Sinan Başaran
Department of Mechanical Engineering
Bilecik Şeyh Edebali University
Bilecik, Türkiye
sinan.basaran@bilecik.edu.tr

***Abstract*— This study focuses on vertical take-off and landing (VTOL) unmanned aircraft, examining the impact of air-launched missile releases on the system. The release process not only disrupts the system's symmetric structure but also alters its mass and inertia parameters. To address these challenges, the study introduces a model to analyze the effects of missile releases and incorporates a wind turbulence model to evaluate aircraft performance under various scenarios.**

***Keywords*— Trajectory control, VTOL, air-launched missile, unsymmetric structure**

I. Introduction

The development of unmanned aerial vehicles (UAVs) has been on the rise in recent years, particularly in the defense industry. Conventional fixed-wing unmanned aircraft are usually equipped with a single propulsion engine. By integrating four additional engines, these systems gain VTOL capability. This design merges the benefits of rotorcraft, such as vertical flight and hovering, with the efficiency and range of fixed-wing aircraft.

VTOL UAV systems have been widely researched across various structures and scales. Critical aspects of this research include evaluating trajectory control performance, developing dynamic models, and examining how changes in system parameters during flight impact the aircraft's trajectory. The dynamics of quadrotors closely resemble those of VTOL UAV systems, a similarity often leveraged in research to progress control strategies tailored for multi-rotor systems. These systems are inherently unstable, making the design of robust control laws a critical focus area [1]. Various control strategies for VTOL UAVs have been explored in the literature. For instance, [2] investigates a stabilization strategy to maintain the UAV's position in crosswinds despite unknown aerodynamic effects. The six-degrees-of-freedom mathematical model of a VTOL aircraft, focusing on forces and moments, was analyzed in [3]. Zou and Meng addressed the coordinated trajectory tracking problem for multiple VTOL UAVs, assuming unidirectional information flow among them [4]. Additionally, Roberts and Tayebi proposed an adaptive position tracking control scheme for VTOL UAVs, designed to handle bounded external disturbances [5]. Study [6] introduced a landing analysis model specifically designed for a short take-off and vertical landing (STOVL) aircraft system, providing insights into its landing dynamics and performance.

This research study explores a fixed-wing air vehicle system with VTOL capabilities, designed for potential military applications and the study is a continuation of the research work carried out in reference [7]. While dynamic models like quadrotors exhibit symmetrical structures in both the -xz and -yz planes, VTOL UAV equipped with missiles on the right and left sides are typically symmetric only in the -xz plane. The release of a missile during flight disrupts this symmetry, leading to changes in the system's inertia tensor and total mass. As a result, the dynamic model must account for these variations to ensure accurate representation of the system's behavior. The study explores a scenario where the UAV conducts a vertical take-off in quadrotor mode and follows a predefined trajectory while subjected to wind disturbances. During flight simulations, at varying intervals, the UAV releases missiles from the left and right sides in succession, allowing the analysis of the system's response to these asymmetrical changes.

II. Aircraft Model

The aircraft structure is shown schematically in Figure 1. The UAV system has four propellers for vertical take-off and one for forward thrust. The vertical take-off propellers are powered by electrical motors, while the forward thrust propeller is driven by a fuel engine. The system initially departs using electrical motors and then transitions to cruise mode, where the internal combustion engine becomes the sole power source. In this UAV system, missile launch is considered in two different scenarios. In the first scenario, the aircraft reaches a fixed altitude and releases the missiles simultaneously. In the second scenario, the aircraft launches one missile during its ascent, and after reaching the fixed altitude, the second missile is released at a later time.

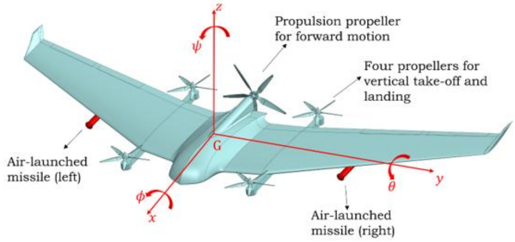

Fig. 1. VTOL unmanned aircraft vehicle model

III. Mathematical Modeling of VTOL UAV

A. *Model of a Quadrotor*

Quadrotors are the most widely used type of VTOL UAVs. To describe both translational and rotational movements, a local coordinate system is assumed at the center of mass. The rotational motions—roll, pitch, and yaw—are represented by the angular variables ϕ, θ and ψ, respectively, around the x, y, and z axes. Due to its symmetrical design, the quadrotor is assumed to exhibit symmetry in the -xz and -yz planes. The rotation matrix that represents the transformation from the local coordinate system to the inertial frame can be expressed as follows:

$$\boldsymbol{R} = \begin{bmatrix} C_\theta C_\psi & S_\theta C_\psi S_\phi - S_\psi C_\phi & S_\theta C_\psi C_\phi + S_\psi S_\phi \\ C_\theta S_\psi & S_\theta S_\psi S_\phi + C_\psi C_\phi & S_\theta S_\psi C_\phi - C_\psi S_\phi \\ -S_\theta & C_\theta S_\phi & C_\theta C_\phi \end{bmatrix} \tag{1}$$

here $C_{\{\}}$ given for the cosine and, $S_{\{\}}$ given for the sine function. A quadrotor's inertia tensor is given as follows because of its symmetrical structure.

$$\boldsymbol{I}_{quad} = \begin{bmatrix} I_{xx} & 0 & 0 \\ 0 & I_{yy} & 0 \\ 0 & 0 & I_{zz} \end{bmatrix} \tag{2}$$

The inertia tensor shows that for a quadrotor, all terms are zero except for the diagonal ones. A quadrotor's translational and rotational dynamic equations can be examined independently. The equation of motion for the quadrotor's translational dynamics is provided by Equation (3).

$$m\ddot{\boldsymbol{\xi}} + mg\boldsymbol{i}_z = \boldsymbol{T} \tag{3}$$

Here, m stands for the quadrotor's total mass, $\boldsymbol{\xi} = [x \quad y \quad z]^T$ is the absolute translational vector of the system, $\boldsymbol{i}_z = [0 \quad 0 \quad 1]^T$ is the gravity related term and $\boldsymbol{T}$ given for thrust. It is possible to define the matrix for angular velocities from the inertial frame to the body frame transformation as given below.

$$\boldsymbol{W_\eta} = \begin{bmatrix} 1 & 0 & -S_\theta \\ 0 & C_\phi & C_\theta S_\phi \\ 0 & -S_\phi & C_\theta C_\phi \end{bmatrix} \tag{4}$$

The Jacobian for the system can be expressed using the transformation that converts coordinates from the inertial frame to the body frame, as given below.

$$\boldsymbol{J} = \boldsymbol{W_\eta^T} \boldsymbol{I}_{quad} \boldsymbol{W_\eta} \tag{5}$$

Equation for system rotational dynamics is given below.

$$\boldsymbol{J}\ddot{\boldsymbol{\eta}} + \boldsymbol{C}(\boldsymbol{\eta}, \dot{\boldsymbol{\eta}})\dot{\boldsymbol{\eta}} = \boldsymbol{\tau}_q \tag{6}$$

Here, $\boldsymbol{\eta} = [\phi \quad \theta \quad \psi]^T$ represents angular position, $\boldsymbol{C}$ stand for the Coriolis matrix with gyroscopic and centripetal expressions [8], and $\boldsymbol{\tau}_q$ represents the torque.

B. *Dynamic of the VTOL Aircraft with Air-launched Missiles*

This study assumes that air-launched missiles mounted on the aircraft's right and left side are released at separate intervals, leading to changes in the aircraft's total mass and inertia tensor during flight. The translational dynamics of the proposed VTOL UAV system are represented as given.

$$m_t\left(\ddot{\boldsymbol{\xi}} + g\boldsymbol{i}_z\right) = \boldsymbol{T} \tag{7}$$

Where m_t is the whole mass of the system which contains the sum of right and left missiles.

$$m_t = m_{UAV} + m_{lm} + m_{rm} \tag{8}$$

The rotational dynamics equation for VTOL UAVs is comparable to the quadrotor system represented in Eq (6).

$$\boldsymbol{J}_v\ddot{\boldsymbol{\eta}} + \boldsymbol{C}_v(\boldsymbol{\eta}, \dot{\boldsymbol{\eta}})\dot{\boldsymbol{\eta}} = \boldsymbol{\tau}_v \tag{9}$$

Here $\boldsymbol{J}_v$ stand for the Jacobian matrix, and $\boldsymbol{C}_v$ denotes the Coriolis matrix, which includes gyroscopic and centripetal expression, similar to those in quadrotor dynamics. The primary distinction between VTOL UAVs and quadrotors lies in how these matrices are derived. For quadrotors, symmetry in both the -xz and -yz planes results in an inertia tensor with only diagonal terms. In contrast, VTOL UAVs are symmetric solely in the -xz plane, and this symmetry is disrupted when air-launched missiles from the right and left wings are released at different times. Consequently, it is essential to develop a dynamic model for the VTOL UAV that accounts for the important scenario where system symmetrical status is no longer maintained.

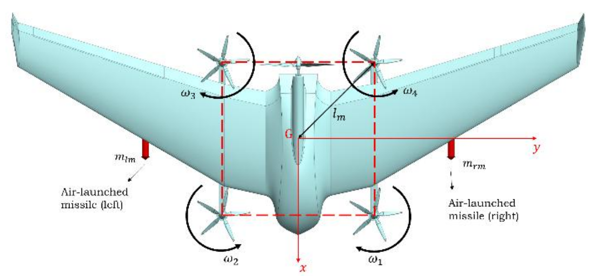

Fig. 2. Top view of the VTOL aircraft model.

Figure 2 illustrates a top view of the VTOL UAV system being studied. As shown, prior to take-off, air-launched missiles m_{lm} and m_{rm} are positioned on the left and right sides. A VTOL UAV system intended for quadrotor operation or trajectory tracking in that mode is the subject of this study. Three different conditions for mass and inertia tensor will arise from the release of these air-launched missiles at various points during the flight. The following sequence is the change in the total mass and inertia tensor.

$$\begin{aligned}
0 < \mathrm{t} < t_1 &\rightarrow \begin{cases} \text{Total Mass} = m_{UAV} + m_{lm} + m_{rm} \\ \boldsymbol{I}_{VTOL} = \begin{bmatrix} I_{xx} & 0 & I_{xz} \\ 0 & I_{yy} & 0 \\ I_{zx} & 0 & I_{zz} \end{bmatrix} \end{cases} \\
t_1 < \mathrm{t} < t_2 &\rightarrow \begin{cases} \text{Total Mass} = m_{UAV} + m_{lm} \\ \boldsymbol{I}_{VTOL} = \begin{bmatrix} I_{xx} & I_{xy} & I_{xz} \\ I_{yx} & I_{yy} & I_{yz} \\ I_{zx} & I_{zy} & I_{zz} \end{bmatrix} \end{cases} \\
t_2 < \mathrm{t} < t_f &\rightarrow \begin{cases} \text{Total Mass} = m_{UAV} \\ \boldsymbol{I}_{VTOL} = \begin{bmatrix} I_{xx} & 0 & I_{xz} \\ 0 & I_{yy} & 0 \\ I_{zx} & 0 & I_{zz} \end{bmatrix} \end{cases}
\end{aligned} \tag{10}$$

where t_f is the total flight time.

C. Euler-Lagrange Equations

This section presents the derivation of the equation of motion for the given system applying the Lagrange method. To implement the dynamic equation, the system's kinetic energy and potential energy are expressed as follows.

$$K_{trans} = \frac{1}{2} m_{UAV} \dot{\boldsymbol{\xi}}^T \dot{\boldsymbol{\xi}}$$
$$U = m_{UAV} g z \tag{11}$$

The translational and vertical dynamics can be derived independently since the UAV's linear and angular components are independent. The provided Lagrange equation is solved using the total kinetic and potential equations.

$$\frac{d}{dt}\left(\frac{\partial K_{trans}}{\partial \dot{\xi}}\right) - \frac{\partial K_{trans}}{\partial \xi} + \frac{\partial U}{\partial \xi} = \boldsymbol{T} \tag{12}$$

Equation (7) provides the translational dynamic equation of the proposed system once the required operations on the Lagrange equation have been completed. The Jacobian matrix can be used to express rotational kinetic energy in order to formulate the system's rotational dynamics, as seen below.

$$K_{rot} = \frac{1}{2} \dot{\boldsymbol{\eta}}^T \boldsymbol{J_v} \dot{\boldsymbol{\eta}} \tag{13}$$

Here, Jacobian matrix able to be described as follows.

$$\boldsymbol{J_v} = \boldsymbol{W_\eta^T} \boldsymbol{I}_{VTOL} \boldsymbol{W_\eta} \tag{14}$$

Additionally, the Jacobian matrix has been computed using the inertia tensor that was found for the scenario in which the system's symmetrical design is disturbed.

$$\boldsymbol{J_v} = \begin{bmatrix} J_{11} & J_{12} & J_{13} \\ J_{21} & J_{22} & J_{23} \\ J_{31} & J_{32} & J_{33} \end{bmatrix} \tag{15}$$

Every component of the Jacobian matrix is given in its most generic symbolic form can be found in reference [7]. The following rotational dynamics is obtained by applying the rotating kinetic energy expression to the provided Lagrange equation.

$$\frac{d}{dt}\left(\frac{\partial K_{rot}}{\partial \dot{\eta}}\right) - \frac{\partial K_{rot}}{\partial \eta} = \boldsymbol{\tau_v} \tag{16}$$

Eq. (9), which provides the rotating equation of the UAV, can be determined by carrying out the required operations in the Lagrange equation. In this case, $\boldsymbol{C_v}(\boldsymbol{\eta}, \dot{\boldsymbol{\eta}})$ stands for the Coriolis matrix, which includes the centripetal and gyroscopic terms.

$$\boldsymbol{C_v} = \begin{bmatrix} C_{11} & C_{12} & C_{13} \\ C_{21} & C_{22} & C_{23} \\ C_{31} & C_{32} & C_{33} \end{bmatrix} \tag{17}$$

The elements of the Coriolis matrix for the case where the UAV is not symmetric are also given in reference [7]. The VTOL UAV's translational and rotational motion equations are provided in Eqs. (7) and (9) here, $\boldsymbol{T} = \boldsymbol{R}[0 \quad 0 \quad T]^T$ represents the total thrust vector, while $\boldsymbol{\tau_q} = [\tau_\phi \quad \tau_\theta \quad \tau_\psi]^T$ denotes the total torque. The rotors of the VTOL UAV seen in Figure 2 are positioned in a cross arrangement. The aircraft's center is where the four rotors are positioned diagonally. Usually, this configuration is selected to improve mobility and aerodynamic performance.

D. Wind Turbulence Model

The Dryden Wind Turbulence Model is a prominent stochastic framework commonly utilized to simulate atmospheric turbulence effects on aircraft, including unmanned aerial vehicles (UAVs). This model mathematically characterizes wind disturbances as a frequency-dependent function, making it a valuable tool for assessing the performance of flight control systems and ensuring stability under diverse wind conditions. The Dryden model is particularly useful for UAVs because it offers a balance between computational efficiency and realistic turbulence representation.

There are specifically created blocks in MATLAB for the Dryden Wind Turbulence Model. These blocks implement the mathematical expressions given from Military Specification MIL-F-8785C, Military Handbook MIL-HDBK-1797, and Military Handbook MIL-HDBK-1797B [9-10]. Based on the military references the turbulence scale lengths at low altitudes are given as follows.

$$L_w = h, \qquad L_u = L_v = \frac{h}{(0.177 + 0.000823h)^{1.2}} \tag{18}$$

Here L_u, L_v, and L_w are represents the turbulence scale lengths in the along-wind, cross wind, and vertical directions. Turbulence scale lengths at low altitudes are represented as

$$\sigma_w = 0.1 W_{20}, \qquad \frac{\sigma_u}{\sigma_w} = \frac{\sigma_v}{\sigma_w} = \frac{1}{(0.177 + 0.000823h)^{0.4}} \tag{19}$$

Here W_{20} is the wind speed at 20 feet (6 m). This value is generally considered for light turbulence conditions and assumes a wind speed of 15 knots for a height of 20 feet. The disruptive external drag force and moment caused by the wind affect the unmanned aerial vehicle during flight. These effects can be implemented into the model as follows [11].

$$F_{wi} = \frac{1}{2} c \rho S_i W_i^2\,, \;\; M_{wi} = \frac{1}{2} c \rho S_i l W_i^2 \;\; (\, i = x, y, z) \tag{20}$$

where ρ is the air density, c represents the drag coefficient, S_i represent the surface area of the aircraft in the region corresponding to the corresponding cross-sectional plane. The wind field created in the simulation model affecting the VTOL aircraft is shown in Figure 3.

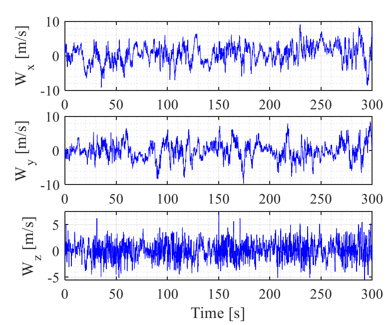

Fig. 3. Generated wind speed components.

IV. Control Simulation of the VTOL UAV Model

In this research, the quadrotor structure is employed as a representative model for the VTOL UAV system. Thanks to its VTOL capability, the aircraft can effectively follow the designated trajectory during takeoff, landing, and flight operations. Table 1 lists the physical characteristics of the VTOL UAV system used in simulation investigation. Designed with a total payload capacity of 8 kilograms, the UAV is assumed to carry two lightweight category 4-kilogram air-launched missiles, one mounted on each wing. For the system's maiden flight scenario, it is anticipated that both missiles will be launched simultaneously at the 200th second within a predefined 300-second trajectory. Additionally, an alternative flight scenario was developed where the right missile is released at the 100th second, then the left missile at the 200th second, within the same 300-second trajectory. This simulation aims to evaluate the effects of staggered missile launches. During the simulations, the wind disturbance illustrated in Figure 3 was applied to the UAV, allowing for an analysis of its impact on both trajectory tracking performance and missile launch dynamics.

Table 1. The VTOL UAV system's parameters, used in simulations.

Parameter	**Definition**	**Value and [unit]**
m	Mass of the UAV	$0 < t < t_1 \rightarrow 40.47$ [kg] $t_1 < t < t_2 \rightarrow 36.47$ [kg] $t_2 < t < t_f \rightarrow 32.47$ [kg]
m_{lm}	Left air-launched missile mass	4 [kg]
m_{rm}	Right air-launched missile mass	4 [kg]
l_m	Distance between rotors and UAV center of mass	0.5 [m]
k	Lift constant	1.2 [-]
b	Drag constant	0.083 [-]

In this study, the VTOL capability is realized using a quadrotor structure, and a comprehensive control design has been developed. A conventional PID controller is employed to manage the trajectory control, with separate controller designs implemented for translational and rotational dynamics. This separation is possible because the dynamics can be handled independently. The simulated control framework is presented in Figure 4 as a Matlab/Simulink model. The VTOL UAV system is classified as an underactuated system, as it has only four actuators to control its desired trajectory, while the system itself possesses six degrees of freedom. The PID controller generates the total thrust vector ($\boldsymbol{T}$) and total torque vector ($\boldsymbol{\tau_v}$) as the system's control inputs. As depicted in Figure 4, the system uses the desired trajectory as its input, while the translational controller determines the required roll and pitch angles necessary for controlling the rotational dynamics.

In the simulations, the inertia tensor of the UAV $\boldsymbol{I}_{VTOL}$, varies over specific time intervals, reflecting dynamic changes in the system's mass distribution and configuration. These variations are implemented to simulate realistic operational scenarios and assess the control system's adaptability under changing conditions.

$$
\begin{aligned}
0 < t < t_1 &\rightarrow \begin{bmatrix} 12.5298 & 0 & 0.0855 \\ 0 & 1.6518 & 0 \\ 0.0855 & 0 & 14.0937 \end{bmatrix} \\
t_1 < t < t_2 &\rightarrow \begin{bmatrix} 10.4760 & 0.3404 & 0.0572 \\ 0.3404 & 1.4343 & 0.1771 \\ 0.0572 & 0.1771 & 11.8535 \end{bmatrix} \\
t_2 < t < t_f &\rightarrow \begin{bmatrix} 8.3268 & 0 & 0.0288 \\ 0 & 1.2168 & 0 \\ 0.0288 & 0 & 9.5178 \end{bmatrix}
\end{aligned} \tag{21}
$$

The chosen PID control gains for managing the translational dynamics of the system are provided below. These gains are specifically tuned to ensure precise trajectory tracking and stability during flight operations.

$$K_{p,t} = 25,\ K_{i,t} = 8,\ K_{d,t} = 110 \tag{22}$$

Similarly, the PID controller gains for the rotation control are provided as follows.

$$K_{p,r} = 2,\ K_{i,r} = 0.1,\ K_{d,r} = 5 \tag{23}$$

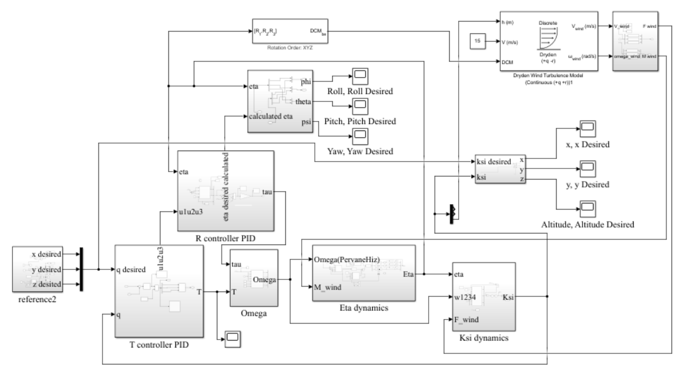

Fig. 4. Matlab/Simulink simulation model.

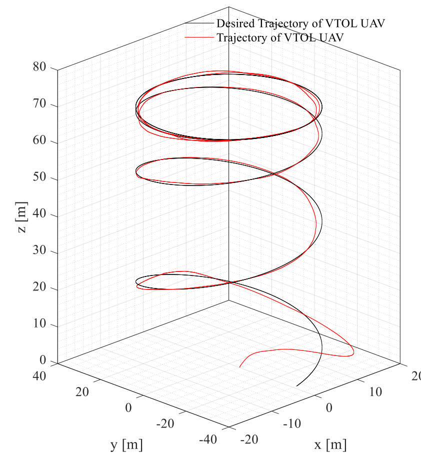

Fig. 5. Desired and actual trajectory of VTOL UAV for releasing the air-launched missiles simultaneously

Figure 5 illustrates that the VTOL UAV system effectively tracks the desired trajectory under PID control during the first flight scenario. Around the midpoint of the total flight duration, at the 180th second, the UAV successfully aligns itself with the intended circular trajectory in the air. At the 200th second, while maintaining this trajectory, the UAV simultaneously releases the left and right air-launched missiles. The simultaneous release of both missiles preserves the system's symmetrical structure; however, the associated mass variations and changes in system parameters can disrupt the target altitude during flight. To analyze this effect more closely, Figure 6 presents the UAV's altitude profile. The missile release induces a temporary disturbance in the system, causing a slight deviation in altitude. As highlighted in the detailed section of Figure 6, the simultaneous release of the missiles results in an approximate deviation of 1.6 meters from the intended trajectory.

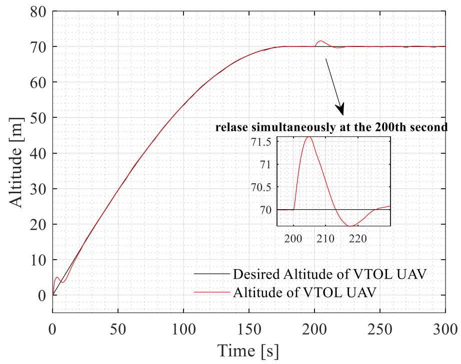

Fig. 6. VTOL's altitude for releasing the air-launched missiles simultaneously.

Along with the air-launched missiles being released simultaneously throughout the flight, staggered missile releases at different times may also align with the mission objectives of the aircraft. To evaluate this, a second flight scenario was analyzed where the missile on the right wing was released at the 100th second, followed by the missile on the left wing at the 200th second. Figure 7 depicts the altitude variations of the UAV for this scenario. As shown, the release of a single air-launched missile exerts a smaller impact on the UAV compared to the simultaneous release of both missiles. Specifically, the individual missile launches cause a trajectory deviation of approximately 0.8 meters. The simulation results further indicate that the system requires a minimum recovery time of 25 seconds to return to the desired trajectory after a missile release. This recovery period ensures a more stable platform for subsequent missile launches, improving accuracy and mission reliability. In addition to trajectory tracking results, the variations in the roll, pitch, and yaw angles during this scenario are illustrated in Figure 8, providing further insights into the system's dynamic response.

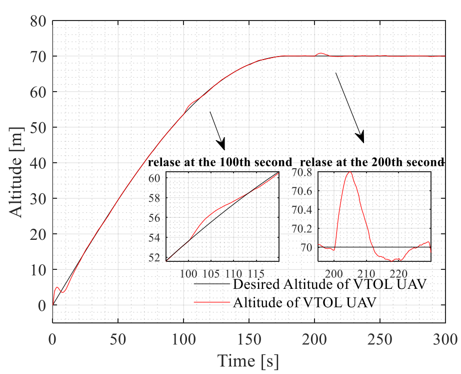

Fig. 7. VTOL's altitude for releasing the air-launched missiles at different times.

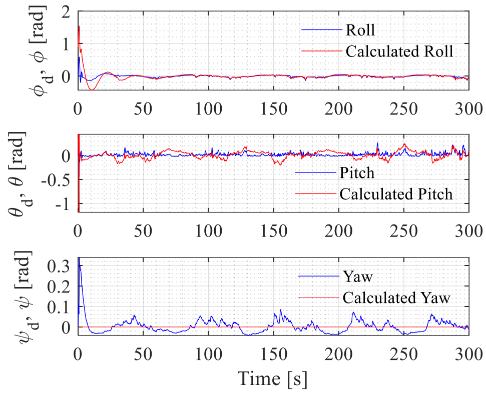

Fig. 8. Variations of roll, pitch and yaw variables

V. CONCLUSIONS

In this study, the effects of rockets fired at different times and simultaneously on the wings of a military UAV VTOL aircraft on the trajectory of the aircraft were investigated. For this purpose, the limits of the model were tested by applying wind loads to the obtained model. In the simulation results, it was observed that the deviations from the trajectory were greater due to the simultaneous release of the missiles. In general, it was found that the effect of the wind on the results was limited and that the stability of the aircraft was not affected.

REFERENCES

[1] Chodnicki, M., Mazur, M., Nowakowski, M. and Kowaleczko,G. (2019), "The mathematical model of UAV vertical takeoff and landing", Aircraft Engineering and Aerospace Technology, Vol. 91No. 2, pp. 249-256.

[2] Pflimlin, J.M., Soueres, P. and Hamel, T. (2007), "Position control of a ducted fan VTOL UAV in crosswind", International Journal of Control. Taylor & Francis, Vol. 80 No. 5, pp. 666-683.

[3] Zhang, J., Guo, Z. and Wu, L. (2017), "Research on control scheme of vertical take-off and landing fixed-wing uav", 2017 2nd Asia-Pacific Conference on Intelligent Robot Systems (ACIRS). IEEE, pp. 200-204.

[4] Zou, Y. and Meng, Z. (2019), "Coordinated trajectory tracking of multiple vertical take-off and landing UAVs", Automatica, Vol. 99, pp. 33-40.

[5] Roberts, A. and Tayebi, A. (2010), "Adaptive position tracking of VTOL UAVs", IEEE Transactions on Robotics, Vol. 27 No. 1, pp. 129-142.

[6] Sivrioglu, S. (2023a), "A landing dynamics analysis model for STOVL aircraft", Proceedings of 10th International Conference on Recent Advances in Air and Space Technologies, RAST 2023, doi: 10.1109/RAST57548.2023.10197967.

[7] Sivrioglu, S. and Basaran, S. (2024), "A vertical take-off and landing (VTOL) unmanned aircraft vehicle trajectory control model with air-launched missiles", Aircraft Engineering and Aerospace Technology, https://doi.org/10.1108/AEAT-04-2024-0118

[8] Luukkonen, T. (2011), "Modelling and control of quadcopter", Independent Research Project in Applied Mathematics, Vol. 22, No. 22.

[9] Park, S., Lee, S., Im, B., Lee, D., & Shin, S. (2023). Improvement of a multi-rotor UAV flight response simulation influenced by gust. Aerospace Science and Technology, 134, 108156.

[10] Tran, N. K. (2015). Modeling and control of a quadrotor in a wind field. McGill University (Canada).

[11] Zeng, Z., Zhi, Y., Hu, H., Liu, L., Fan, H., & Wang, B. (2023, July). Modeling and Control for Quadrotor Aircraft Subject to Wind Gusts. In 2023 42nd Chinese Control Conference (CCC) (pp. 2376-2381). IEEE.